

AD-A142 525

OPTICAL SUPPORT HARTMANN SENSOR OPTICAL SIMULATION(U)  
UNITED TECHNOLOGIES OF NEW MEXICO INC EAST HARTFORD CT  
J L FORGHAM ET AL. MAY 84 AFWL-TR-83-115

1/1

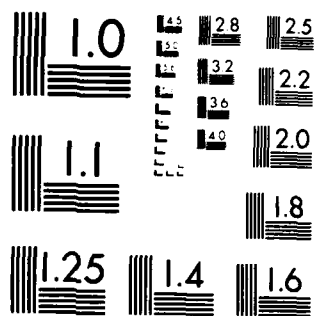
UNCLASSIFIED

F29601-83-C-0023

F/G 20/6

NI

						END							
						DATE							
						FILED							
						8 84							
						DTIC							



MICROCOPY RESOLUTION TEST CHART  
NATIONAL BUREAU OF STANDARDS 1963-A

2

AFWL-TR-83-115

AFWL-TR-  
83-115

AD A142525

## OPTICAL SUPPORT HARTMANN SENSOR OPTICAL SIMULATION

James L. Forgham  
Harold D. McIntire

United Technologies of New Mexico, Inc  
Silver Lane  
East Hartford CT 06108

May 1984



Final Report

Approved for public release; distribution unlimited.

DTIC FILE COPY

AIR FORCE WEAPONS LABORATORY  
Air Force Systems Command  
Kirtland Air Force Base, NM 87117

DTIC  
ELECTE  
JUN 25 1984  
S E D

84 06 22 035

This final report was prepared by the United Technologies of New Mexico, Inc, East Hartford, Connecticut, under Contract F29601-83-C-0026, Job Order 39391904 with the Air Force Weapons Laboratory, Kirtland Air Force Base, New Mexico. Lieutenant Jill L. Rider (ARLB) was the Laboratory Project Officer-in-Charge.

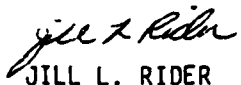
When Government drawings, specifications, or other data are used for any purpose other than in connection with a definitely Government-related procurement, the United States Government incurs no responsibility or any obligation whatsoever. The fact that the Government may have formulated or in any way supplied the said drawings, specifications, or other data, is not to be regarded by implication, or otherwise in any manner construed, as licensing the holder, or any other person or corporation; or conveying any rights or permission to manufacture, use, or sell any patented invention that may in any way be related thereto.

This report has been authored by a contractor of the United States Government. Accordingly, the United States Government retains a nonexclusive, royalty-free license to publish or reproduce the material contained herein, or allow others to do so, for the United States Government purposes.

This report has been reviewed by the Public Affairs Office and is releasable to the National Technical Information Services (NTIS). At NTIS, it will be available to the general public, including foreign nations.

If your address has changed, if you wish to be removed from our mailing list, or if your organization no longer employs the addressee, please notify AFWL/ARLB, Kirtland AFB, NM 87117 to help us maintain a current mailing list.

This technical report has been reviewed and is approved for publication.

  
JILL L. RIDER  
Lieutenant, USAF  
Project Officer

  
ROBERT L. VAN ALLEN  
Maj, USAF  
Chief, Systems Development Branch

FOR THE COMMANDER

  
DENNIS L. BOESEN  
Lt Colonel, USAF  
Chief, Laser Development Division

DO NOT RETURN COPIES OF THIS REPORT UNLESS CONTRACTUAL OBLIGATIONS OR NOTICE ON A SPECIFIC DOCUMENT REQUIRES THAT IT BE RETURNED.

UNCLASSIFIED

SECURITY CLASSIFICATION OF THIS PAGE

## REPORT DOCUMENTATION PAGE

1a. REPORT SECURITY CLASSIFICATION <b>Unclassified</b>			1b. RESTRICTIVE MARKINGS		
2a. SECURITY CLASSIFICATION AUTHORITY			3. DISTRIBUTION/AVAILABILITY OF REPORT Approved for public release; distribution unlimited.		
2b. DECLASSIFICATION/DOWNGRADING SCHEDULE					
4. PERFORMING ORGANIZATION REPORT NUMBER(S)			5. MONITORING ORGANIZATION REPORT NUMBER(S) AFWL-TR-83-115		
6a. NAME OF PERFORMING ORGANIZATION United Technologies of New Mexico, Inc		6b. OFFICE SYMBOL (If applicable)	7a. NAME OF MONITORING ORGANIZATION Air Force Weapons Laboratory		
6c. ADDRESS (City, State and ZIP Code) Silver Lane East Hartford, CT 06108			7b. ADDRESS (City, State and ZIP Code) Kirtland Air Force Base, NM 87117		
8a. NAME OF FUNDING/SPONSORING ORGANIZATION		8b. OFFICE SYMBOL (If applicable)	9. PROCUREMENT INSTRUMENT IDENTIFICATION NUMBER F29601-83-C-0023		
8c. ADDRESS (City, State and ZIP Code)			10. SOURCE OF FUNDING NOS.		
			PROGRAM ELEMENT NO. 63605F	PROJECT NO. 3939	TASK NO. 19
			WORK UNIT NO. 04		
11. TITLE (Include Security Classification) OPTICAL SUPPORT - HARTMANN SENSOR OPTICAL SIMULATION					
12. PERSONAL AUTHOR(S) James L. Forgham, Harold D. McIntire					
13a. TYPE OF REPORT Final Report		13b. TIME COVERED FROM Aug 83 TO Oct 83		14. DATE OF REPORT (Yr., Mo., Day) 1984 May	
15. PAGE COUNT 32					
16. SUPPLEMENTARY NOTATION					
17. COSATI CODES			18. SUBJECT TERMS (Continue on reverse if necessary and identify by block number)		
FIELD 20	GROUP 05	SUB. GR.	Optical Computer Simulation, Optical Sensor, Hartmann Sensor, Hartmann Plate, Aberration, Reconstructed Wavefronts, Phase Reconstruction, Optical Field Generation, Propagation, (over)		
19. ABSTRACT (Continue on reverse if necessary and identify by block number) This report describes the development and validation of a computer simulation of Hartmann sensor optical performance. A brief study was performed using the validated code to evaluate the sensitivity of Hartmann sensor performance to sensor design parameters and input beam aberration characteristics. Significant loss of aberration mode fidelity can result from failure to account for the effects of partially illuminated Hartmann plate subapertures. Such mode fidelity degradations tend to be less severe with moderately high resolution plate designs (e.g., 12 x 12).					
20. DISTRIBUTION/AVAILABILITY OF ABSTRACT UNCLASSIFIED/UNLIMITED <input type="checkbox"/> SAME AS RPT. <input checked="" type="checkbox"/> OTIC USERS <input type="checkbox"/>			21. ABSTRACT SECURITY CLASSIFICATION Unclassified		
22a. NAME OF RESPONSIBLE INDIVIDUAL Lt Rider			22b. TELEPHONE NUMBER (Include Area Code) (505) 844-2986		22c. OFFICE SYMBOL ARLB

UNCLASSIFIED

SECURITY CLASSIFICATION OF THIS PAGE

18. SUBJECT TERMS (Continued)

Phase Analysis, Geometric Optical Model, Wave Optics Model

UNCLASSIFIED

SECURITY CLASSIFICATION OF THIS PAGE

## TABLE OF CONTENTS

<u>Section</u>	<u>Page</u>
I. INTRODUCTION . . . . .	1
II. CODE DEVELOPMENT . . . . .	3
III. CODE VALIDATION . . . . .	4
IV. PARAMETRIC STUDY . . . . .	18
V. CONCLUSIONS . . . . .	25
VI. RECOMMENDATIONS . . . . .	27

Accession For	
NTIS GRA&I	<input checked="" type="checkbox"/>
DTIC TAB	<input type="checkbox"/>
Unannounced	<input type="checkbox"/>
Justification	
By	
Distribution/	
Availability Codes	
Dist	Avail and/or Special
A-1	



## I. INTRODUCTION

It is axiomatic that accurate wavefront aberration measurements are indispensable in the performance evaluation of laser optical systems. However, the diagnostic instruments used to obtain wavefront estimates don't give direct measurements of wavefront optical path differences (OPDs). What can actually be measured are the effects of the aberration, rather than the aberration itself.

In the case of an interferometer, the measurement takes the form of an interference pattern representing wavefront surface contours in specific increments of wavelength. Conversion of this information into an OPD estimate depends upon some numerical algorithm to reconstruct the wavefront from its contour curves.

For a Hartman-type sensor, the measured quantities are subaperture focal spot displacements in a detector plane. These displacements are related to near field local wavefront gradients, which must then somehow be integrated in order to reconstruct the wavefront.

Even in such advanced diagnostic instruments as the heterodyne interferometer, the actual measured quantities are not OPDs but (as the name suggests) return-signal phase differences between two beams of differing frequency. The measured phase difference is then converted to OPD by an internal algorithm which must account for the  $2\pi$ -ambiguity inherent in such conversions.

In any case, the accuracy of the wavefront estimate depends not only upon the accuracy of the measuring instrument, but also upon the fidelity of the numerical process used to convert the raw measurement into the wavefront estimate. In the case of the Hartmann sensor, the spatial filtering characteristics of the lenslet plate also impose a limit on the attainable accuracy.



This report describes the development and validation of a computer simulation of Hartmann sensor performance, together with the results of an abbreviated parametric study performed using the completed and validated simulation code. The report is divided into five sections. Section II summarizes the code development effort. Section III describes the code validation process and presents the results of the validation test cases. Section IV discusses the scope and content of the parametric study. Section V provides some recommendations, based on the results of this effort, for additional areas in which further code development could significantly enhance both this Hartman sensor simulation and other areas of computer analysis and simulation.

## II. CODE DEVELOPMENT

### 1. INITIAL CODE STATUS

The Hartmann sensor simulation code developed under this effort is acutally an extension to and a completion of the simulation code initiated by United Technologies of New Mexico (UTNM) under the fixed price, level-of-effort contract F29601-82-C-0102, "Pointing and Tracking Modeling", acting as a subcontractor to Applied Technology Associates, Inc. The simulation code consisted of an executive program and 55 supporting routines, organized functionally into six modules: Initialization/Control, Field Generation, Propagation, Phase Analysis, Output, and Graphics. The entire simulation was built around two basic models (geometric and wave optics) of Hartmann array optical performance. At the completion of the allocated level-of-effort for the earlier task, approximately 95 percent of the anticipated required code was installed, and the code was about 75 percent checked out.

### 2. EXTENSIONS AND MODIFICATIONS

In this code development effort, the basic structure and modeling approach of the earlier Hartmann simulation code has been preserved. There are still the same six functional modules and the code is still built around the geometric and wave optics models. However, a number of new subroutines have been added in order to meet new computational requirements and provide some expanded outputs. Consolidation of certain computational functions also resulted in a slight increase in the number of subroutines, but eliminated some redundancy of code. In its present configuration, the code consists of the executive program and 71 supporting subroutines, including the phase reconstruction algorithm provided to UTMN by the Air Force Weapons Laboratory (AFWL).

## III. CODE VALIDATION

## 1. FORMAL VALIDATION TEST CASES

The contract Statement of Work (SOW) details three specific test cases for validation of the Hartmann simulation code. This section describes each of these validation test cases in terms of the SOW requirements, the necessary inputs to the code, and the pertinent results.

a. Tilt/Focus Validation Case

(1) Requirements — The specifications set forth in paragraph 4.1.1.2.1.1 of the contract SOW are as follows: "For a phase front composed of one wave ( $\lambda = 0.5$  microns) each of tilt and focus, the net wavefront tilt over each subaperture of a  $3 \times 3$  contiguous array as determined in the code, shall be compared with the analytical solution. The results shall agree within 5 percent".

(2) Description of Inputs — Figure 1 shows the basic geometry for this validation test case. The subapertures have 4-cm radii and the input beam has a radius of 12 cm. The input Zernike coefficients are  $p_3$  (y - tilt) = 1.0 and  $p_4$  (focus) = 1.0. The Zernike polynomial scaling is such that a coefficient of 1.0 corresponds to a maximum amplitude of one-half wave over the normalization aperture (in most cases this is equivalent to a total variation of one wave over the aperture).

(3) Results

(a) Subaperture Net Wavefront Tilts — The analytic form of the input wavefront aberration functions for this case is

$$\phi(x,y) = \frac{x^2 + y^2}{r_n^2} - 1/2 + \frac{y}{2r_n} \quad (1)$$

The analytic expressions for the gradient are then

$$\frac{\partial \phi}{\partial x}(x,y) = \frac{2x}{r_n^2} \quad (2)$$

and

$$\frac{\partial \phi}{\partial y}(x,y) = \frac{2y}{r_n^2} + \frac{1}{2r_n} \quad (3)$$

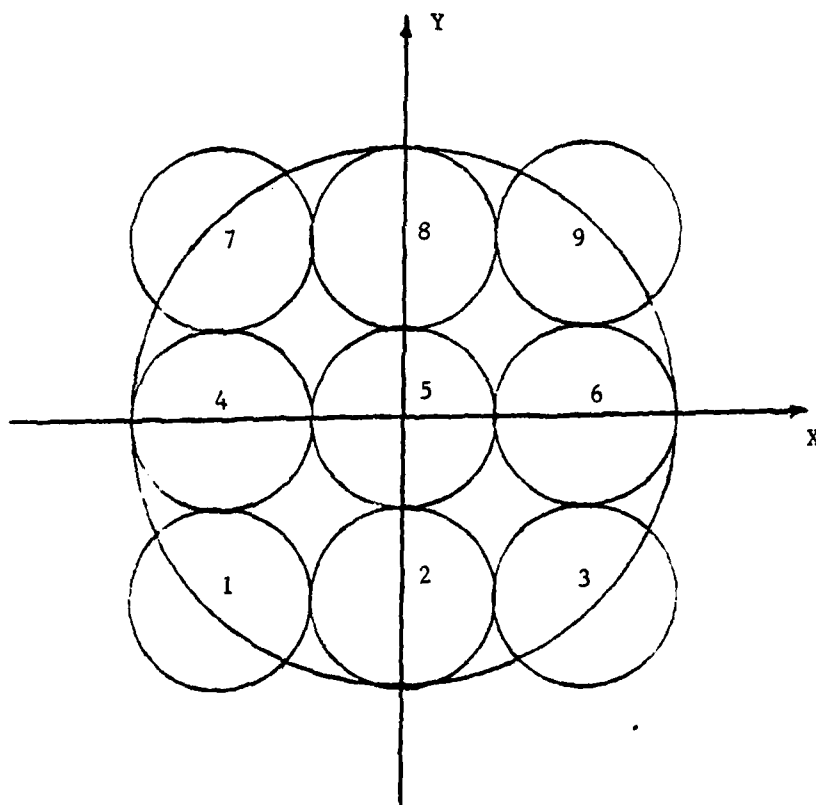


Figure 1. Hartmann 3 X 3 array geometry.

Table 1 compares the functional values of the expressions (Eq. 2, 3) for  $r_n = 12$  with the corresponding values computed by the Hartmann code for both the geometric optics and wave optics models. In both models, the actual numerical processes correspond to computing an average gradient over the illuminated portion of each subaperture. The wave optics model exhibits very slight asymmetries and tends to produce slightly larger errors than does the geometric model. Even so, the worst error is less than 1.1 percent, more than a factor of four below the 5 percent criterion. The worst error for the geometric model is less than 0.2 percent, down a factor of more than 25 from the 5 percent limit.

(b) Other results of interest — The gradient criterion discussed above was the only specification given in the SOW for this validation test case. However, some other results are also of interest in understanding and evaluating the performance of the Hartmann simulation code. Table 2 gives a comparison of the input and output Zernike coefficients through  $p_4$ . The output coefficients labeled "Compensated" are derived using a gradient fitting technique in which each net subaperture gradient is assigned the coordinates of the centroid of illumination for that subaperture. Thus, the procedure compensates for partially illuminated subapertures. The output Zernike coefficients labeled "Uncompensated" are similarly derived, except that the net subaperture gradients are treated as if they occurred at the subaperture geometric centers, irrespective of fractional illumination. As may be seen from the table, the uncompensated procedure (for this  $3 \times 3$  contiguous array geometry) results in errors in the computed  $p_4$  (focus) term on the order of 8 percent to 8.5 percent. In contrast, the errors for the compensated procedure are about 0.1 to 0.4 percent.

Finally, some preliminary inferences may be made regarding the performance of the phase reconstruction algorithm employed in the Hartmann code. This algorithm (like most phase gradient and phase difference algorithms) is structured to reconstruct phase on a uniform square grid from gradient data

TABLE 1. ANALYTIC AND COMPUTED GRADIENTS

Sub- aperture No.	Centroid		Analytic		Geometric model		Wave optics model	
	x	y	$\partial\phi/\partial x$	$\partial\phi/\partial y$	$\partial\phi/\partial x$	% err	$\partial\phi/\partial x$	% err
1	-7.0	-7.0	-0.0972	-0.0556	-0.0971	-0.10	-0.0978	0.62
2	0.0	-8.0	0.0	-0.0694	*	*	*	-0.0691
3	7.0	-7.0	0.0972	-0.0556	0.0971	-0.10	-0.0979	0.72
4	-8.0	0.0	-0.1111	0.0417	-0.1109	-0.19	-0.1107	-0.36
5	0.0	0.0	0.0	0.0417	*	*	*	0.0417
6	8.0	0.0	0.1111	0.0417	0.1109	-0.19	0.1108	-0.27
7	-7.0	7.0	-0.0972	0.1389	-0.0971	-0.10	-0.0978	0.62
8	0.0	8.0	0.0	0.1528	*	*	*	0.1524
9	7.0	7.0	0.0972	0.1389	0.0971	-0.10	0.0978	0.62

\* Absolute error  $< 10^{-4}$ ; % error meaningless with zero base.

TABLE 2. INPUT AND OUTPUT ZERNIKE COEFFICIENTS

Zernike term	Input	Compensated			Uncompensated		
		Geomdl	% err	Wavmdl	% err	Wavmdl	% err
2	0.0	*	*	*	*	*	*
3	1.0	0.9999	-0.01	1.000	0.0	1.000	0.0
4	1.0	1.001	0.1	1.004	0.4	0.9190	-8.1

\* Absolute coefficients  $< 10^{-3}$ ; % error meaningless with zero base.

also given on a uniform square grid. In the presence of partially illuminated subapertures, the phase gradient data used are not really representative of a square grid, thus abusing the algorithm to some extent. On the other hand, these results should be fairly representative of simple Hartmann devices, which normally do not measure near field subaperture irradiance centroids. Table 3 compares analytically determined phase (from Eq. 1) with numerically reconstructed phase from the gradient data for both the geometric and wave optics models. Because the gradient data are devoid of any piston information, the phase reconstructions generally contain a piston error. For purposes of the presentation in the table, a piston correction term was chosen using the average error taken only over the fully illuminated subapertures. The "adj" column in the table reflects the residual wavefront reconstruction error after the piston correction is applied. As expected, significant errors occur in the reconstructed wavefront on partially illuminated subapertures. These effects may be strong contributors to the Zernike mode cross-coupling behavior which has been observed in gradient-phase reconstruction techniques. The significant improvement achieved in the Zernike polynomial fits by compensating for partial subaperture illumination suggests that similar improvements in phase reconstruction fidelity may be possible with a more general algorithm which is not tied to a uniform square data grid. Such a generalized algorithm, coupled with a device for sensing near field subaperture illumination, might potentially provide a significant improvement in the accuracy of Hartmann-type wavefront sensors.

b. Geometric Model Validation Case

(1) Requirements — The specifications set forth in paragraph 4.1.1.2.1.2 of the contract SOW are as follows: "A wavefront composed of low-order Zernike coefficients corresponding to an inviscid flow only condition, and supplied by the government, shall be sampled on a 6 x 6 contiguous array Hartmann plate. The analysis shall use a geometric (tilt only) propagation. The resulting Zernike coefficients derived from the reconstructed wavefront



TABLE 3. ANALYTIC AND RECONSTRUCTED PHASE

Sub- aperture No.	Center		Analytic	Geometric		Wave optics			
	x	y	$\phi$	$\phi$	err	adj <sup>1</sup> 3	$\phi$	err	adj <sup>2</sup> 3
1	-8.0	-8.0	0.0556	-0.0677	-0.123	-0.056	-0.0665	-0.122	-0.054
2	0.0	-8.0	0.3889	0.4563	-0.067	0.0	-0.4577	-0.069	-0.001
3	8.0	-8.0	0.0556	-0.0726	-0.128	-0.061	-0.0711	-0.127	-0.059
4	-8.0	0.0	-0.0556	-0.1221	-0.067	0.0	-0.1235	-0.068	0.0
5	0.0	0.0	-0.5000	-0.5657	-0.066	0.001	-0.5662	-0.066	0.002
6	8.0	0.0	-0.0556	-0.1227	-0.067	0.0	-0.1237	-0.068	0.0
7	-8.0	8.0	0.7222	0.5974	-0.125	-0.058	0.5987	-0.124	-0.056
8	0.0	8.0	0.2778	0.2109	-0.067	0.0	0.2098	-0.068	0.0
9	8.0	8.0	0.7222	0.5988	-0.123	-0.056	0.6003	-0.122	-0.054

## NOTES:

<sup>1</sup> Adjusted by piston term of + 0.067 waves<sup>2</sup> Adjusted by piston term of + 0.068 waves<sup>3</sup> Error values in this table are given in units of waves. They are not % errors.

shall be compared with each known input coefficient and agree within 10 percent. In a case where the criterion cannot be met, the contractor shall submit to the government a written request to waive the criterion for that specific case. The government will respond in writing to all such requests."

(2) Description of Inputs — Figure 2 shows the basic geometry for this validation test case. The input beam still has a 12-cm radius, but the subaperture radius is reduced to 2 cm.

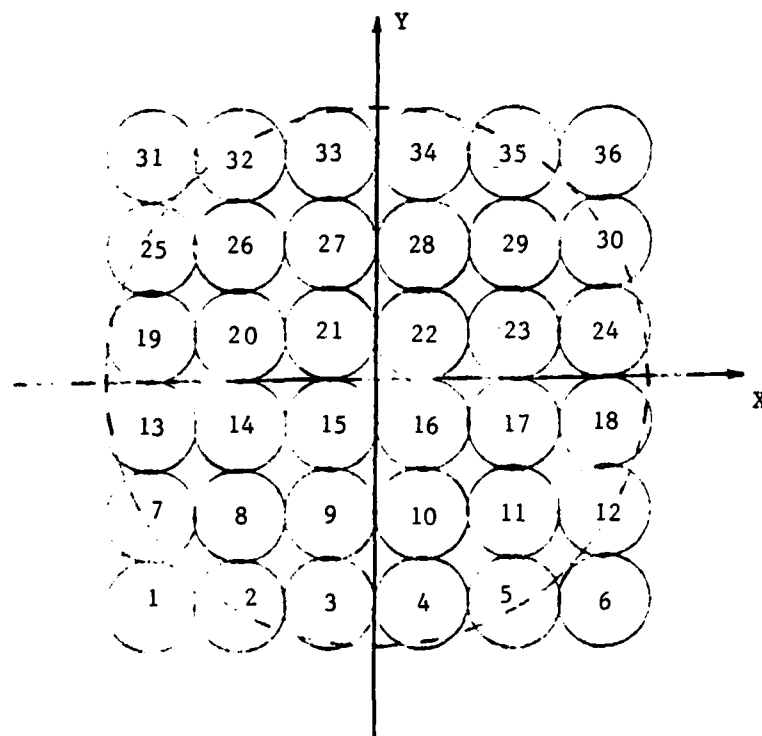


Figure 2. Contiguous 6 X 6 Hartmann array.

(3) Results — Table 4 gives the input and output Zernike coefficients, together with computed percent errors. The input coefficients were provided by AFWL. For these low-order Zernikes, even the uncompensated

TABLE 4. GEOMETRIC MODEL ZERNIKE RESULTS

Zernike term	Input	Compensated			Uncompensated		
		Geomdl	% err	Wavmdl	% err	Wavmdl	% err
2	4.495	4.470	0.56	4.471	-0.53	4.487	-0.18
3	0.0	*	*	*	*	*	*
4	-0.6100	-0.6101	0.02	-0.6087	-0.21	-0.5924	-2.9
5	0.0310	0.0310	0.0	0.0310	0.0	0.0302	-2.5
6	0.0	*	*	*	*	*	*
7	0.3160	-0.3151	-0.28	-0.3148	0.38	-0.2867	-9.3
8	0.0	*	*	*	*	*	*

\* Absolute error  $< 10^{-3}$ ; % error meaningless with zero base.

procedure satisfies the 10 percent criterion specified in the SOW. However, the coefficients determined by the compensated procedure reproduce the input to within about 0.5 percent.

c. Wave Optics Model Validation Case

(1) Requirements — Paragraph 4.1.1.2.1.3 of the contract SOW specifies: "For the input wavefront described in 4.1.1.2.1.2, a comparison shall be made between the geometric and wave optics methods used in the code. This shall be done by comparing the derived coefficients. In the absence of severe point spread function distortion, i.e., by reducing the size of the subaperture, the two methods shall produce coefficients which agree within 5 percent."

(2) Description of Inputs — This case is identical to the case described in Subsection 1b with the exception that the Hartmann array need not be contiguous. That is, the dilution ratio of the array may be treated as a free parameter in meeting the criterion of agreement between the geometric and wave optics models to within 5 percent.

(3) Results — Since the wave optics model was involved in the Subsection 1b case, those results may be used to demonstrate compliance with the requirements for the test case. Table 5 shows that the agreement is well within 5 percent. For comparison, a second run was made, using a dilution ratio of 50 percent. That is, the subaperture radii were reduced to 1 cm. Figure 3 illustrates the geometry and Table 6 shows the results, which are also within the specified 5 percent limit, except for the uncompensated  $p_5$  coefficient.

TABLE 5. ZERNIKE COMPARISON, 6 x 6 CONTIGUOUS ARRAY

Zernike term	Compensated			Uncompensated		
	Geomdl	Wavmdl	% dif	Geomdl	Wavmdl	% dif
2	4.470	4.471	0.02	4.486	4.487	0.02
3	*	*	*	*	*	*
4	-0.6101	-0.6087	0.23	-0.5940	-0.5924	-0.27
5	0.03102	0.3100	-0.06	0.03019	0.03015	-0.13
6	*	*	*	*	*	*
7	-0.3151	-0.3148	-0.10	-0.2870	-0.2867	-0.10
8	*	*	*	*	*	*

\* Absolute coefficients  $< 10^{-3}$ ; % difference not meaningful.

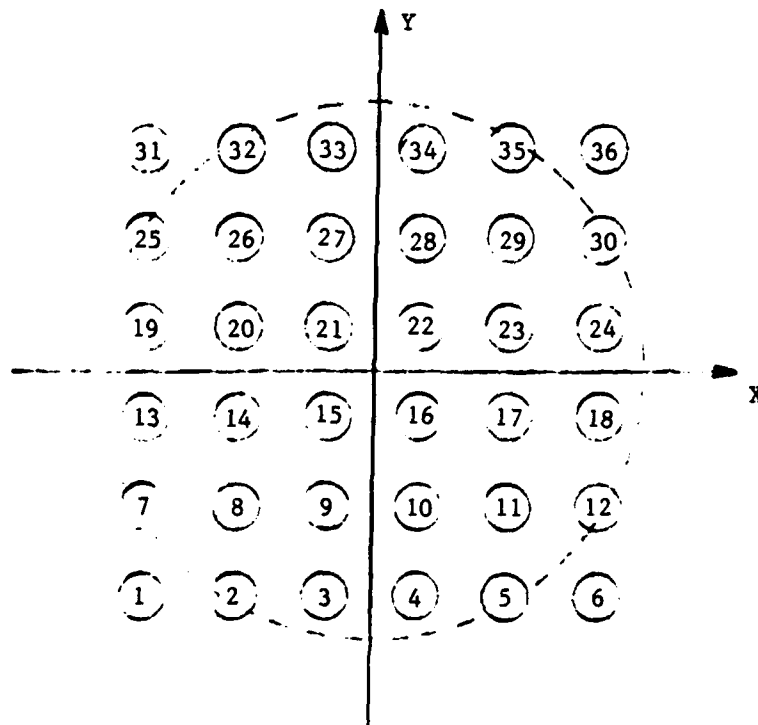


Figure 3. Hartmann 6 X 6 array, 50% dilution.

TABLE 6. ZERNIKE COMPARISON, 6 x 6 ARRAY, 50% DILUTION

Zernike term	Compensated			Uncompensated		
	Geomdl	Wavmdl	% dif	Geomdl	Wavmdl	% dif
2	4.489	4.489	0.0	4.494	4.495	0.02
3	*	*	*	*	*	*
4	-0.6100	-0.6043	-0.93	-0.6044	-0.5986	-0.96
5	0.03101	0.03254	4.9	0.03071	0.03225	5.0
6	*	*	*	*	*	*
7	-0.3159	-0.3156	-0.09	-0.3056	-0.3054	-0.07
8	*	*	*	*	*	*

\* Absolute coefficients  $<10^{-3}$ ; % difference not meaningful.

#### d. Code Performance

The Hartmann sensor simulation code meets the requirements established in the three validation test cases specified in the contract SOW.

The gradient-based Zernike polynomial fitting and phase reconstruction techniques employed in the Hartmann code appear to perform well, with the exception of edge effects which are due to partially illuminated subapertures. Since the Zernike fitting algorithm is a least-squares technique, it was a simple matter to generalize it to compensate for these effects. However, some considerable effort would be required in order to generalize the phase reconstruction algorithm.

## 2. OTHER PERFORMANCE TESTS

a. Propagation — The wave optics propagation algorithm used in the Hartmann simulation code was derived from the far field propagation portions of the Chemical Laser Optical Quality (CLOQ) code, which is a variant of the

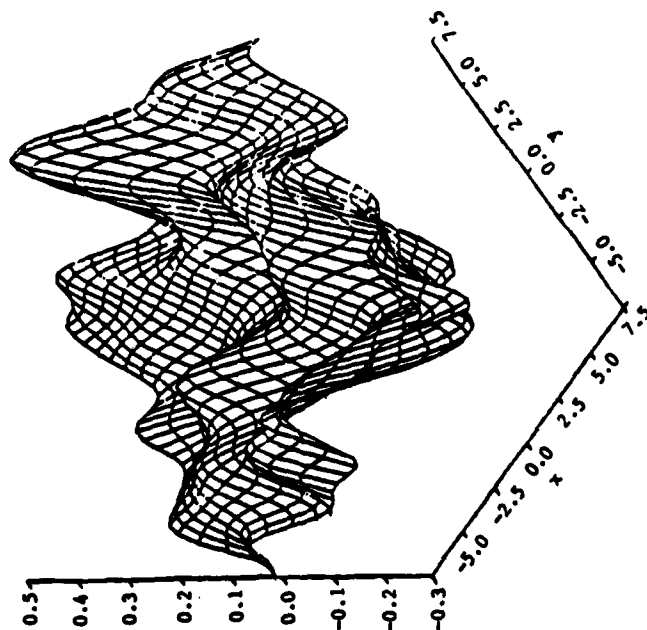
System Optical Quality (SOQ) code. The SOQ code was developed for AFWL by United Technologies as the principal physical optics analysis tool for studies and performance evaluation of the Airborne Laser Laboratory (ALL) resonator and optical train. The SOQ code has been in active use at AFWL since 1973 and is thoroughly validated.

Single-aperture propagation results from the Hartmann code have been compared with both CLOQ and SOQ results using 32 x 32 point calculation grids. The results agree extremely well. For example, for an input plane wave beam with up to one wave of misfocus applied, the total far field power calculated by the three codes differed by less than 0.2 percent.

b. Correlated Random Phase — A principal feature of the Hartmann code is the modeling of phase aberrations due to turbulence effects in atmospheric propagation. Such turbulence effects are modeled in the code as a correlated random phase component generated from user-specified parameters describing the strength and correlation properties of the turbulence. Statistics of the Hartmann sensor performance are compiled from its responses to a sequence of such random phase realizations.

The Hartmann code employs Fast Fourier Transform (FFT) numerical techniques in the generation of correlated random phase. As a built-in check on the actual correlation properties produced, the Hartmann code back-computes the autocorrelation of each specific random phase realization. The average autocorrelation function over the sequence of realizations is then compared with the user-specified correlation function. These comparisons show a slight systematic spreading in the achieved correlation function relative to the specified desired correlation function. Although no detailed analysis of this effect has been performed, it appears that the small observed spreading is inherent in the FFT-based convolution used in the smoothing process. Figure 4 shows a sample three-dimensional and contour plot of a correlated random phase realization.

INPUT PHASE



INPUT PHASE

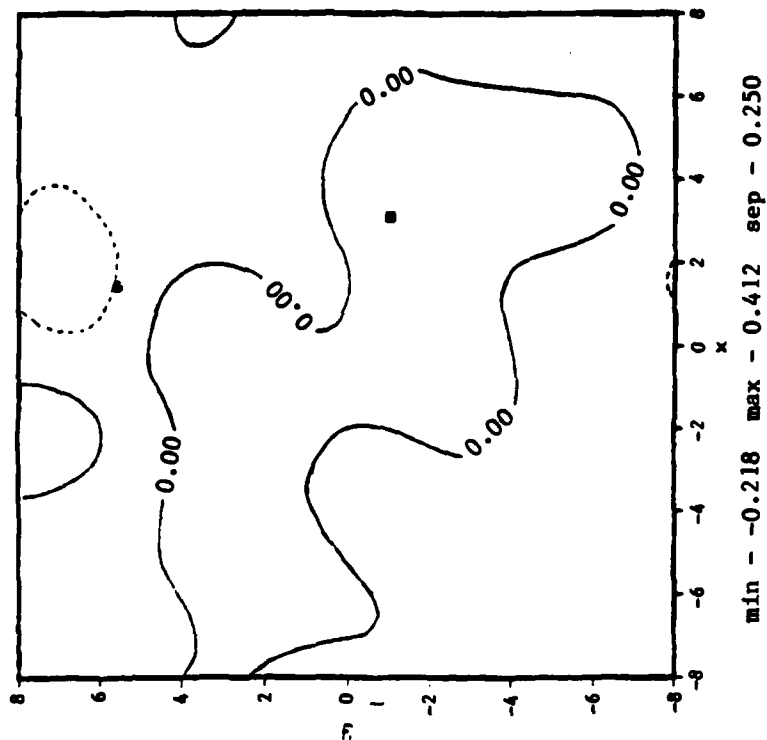


Figure 4. Correlated random phase.



## IV. PARAMETRIC STUDY

## 1. ZERNIKE MODE FIDELITY

A question which is of both theoretical and practical interest is the accuracy with which a Hartmann-type sensor, with its inherent spatial filtering properties, can reproduce specified input Zernike phase modes. There are two facets to this questions. First, for an input phase aberration consisting of a single Zernike mode, how much of that aberration does the sensor think it sees? Second, how much of the Zernike aberrations not present in the input does the sensor think it sees? That is, if the input phase is given by

$$\phi(x,y) = p_k z_k(x,y)$$

where  $z_k$  is the  $k$ th Zernike polynomial, and the output (reconstructed) phase is described by

$$\tilde{\phi}(x,y) = \sum_{i=1}^n \tilde{p}_i z_i(x,y)$$

then the ratio  $\tilde{p}_k/p_k$  represents

the fidelity with which the sensor reproduces the  $k$ th Zernike mode. The ratios  $\tilde{p}_i/p_k$  ( $i \neq k$ ) represent the  $i$ th Zernike mode cross-coupling in the sensor. For a perfect sensor, of course, the fidelity would be 1.0 for each Zernike mode and all cross-coupling terms would be zero.

a. Unobscured Case — Test cases were run using the Hartmann code to investigate the fidelity and cross-coupling properties of 6 x 6, 9 x 9, and 12 x 12 element Hartmann arrays for 8 Zernike modes ranging from  $z_2$  to  $z_{14}$ . Figure 5 shows the fidelity and cross-coupling results for coma ( $p_7$ ). Two trends are fairly clear: (1) Increasing resolution of the Hartmann array tends to improve fidelity and reduce cross-coupling; and (2) the Zernike fitting algorithm which compensates for partially illuminated subapertures has better

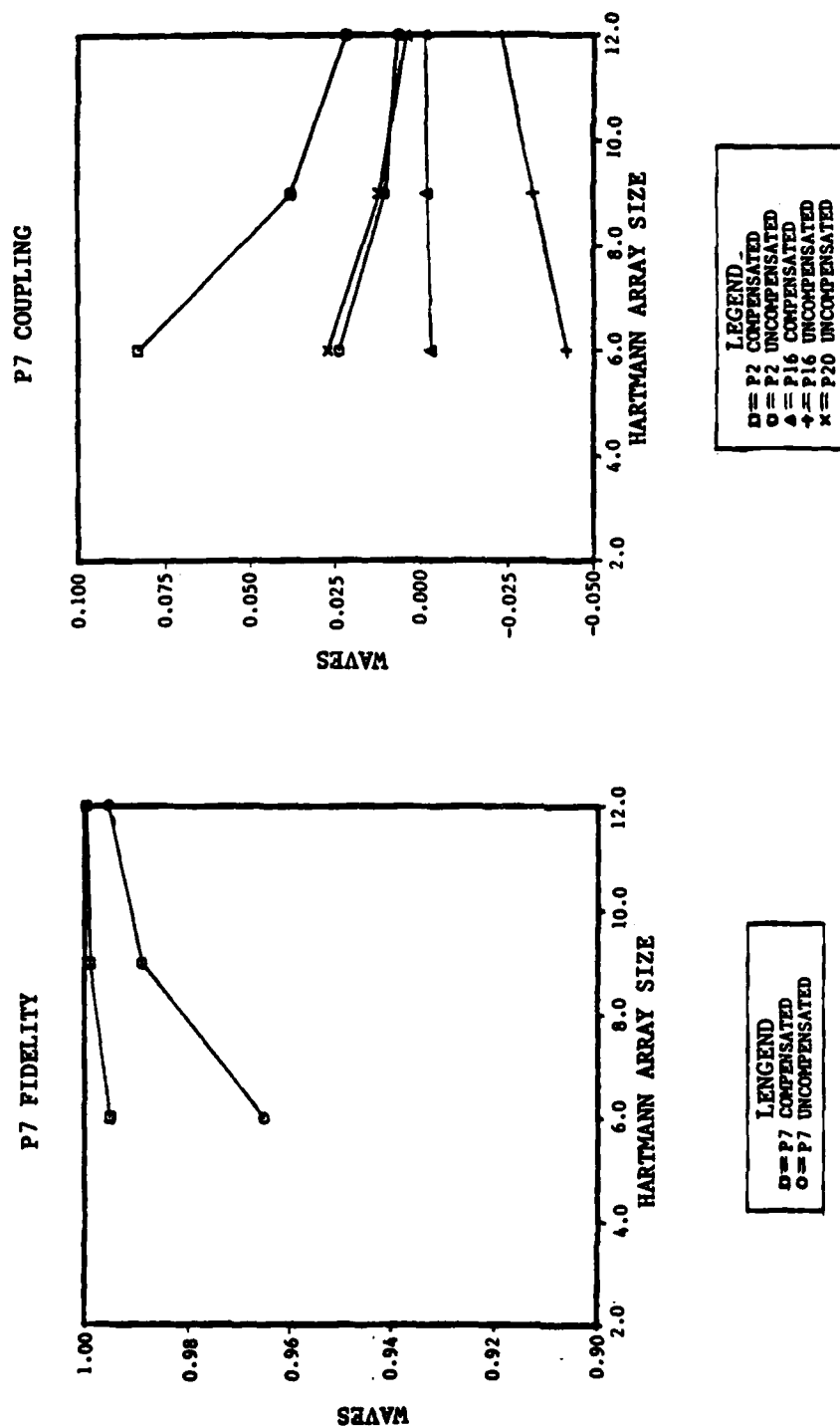


Figure 5. P7 fidelity and cross-coupling.

fidelity and less cross-coupling than the uncompensated algorithm. These results are qualitatively typical of the corresponding results for most other Zernike modes.

b. Obscuration Effects — A few test cases were run for low order Zernike aberrations with central obscurations applied to the input beam. Figure 6 shows the effect of the obscuration ratio on the fidelity and cross coupling for focus ( $p_4$ ). As expected, the compensated Zernike fits are far less sensitive to the central obscuration ratio than are uncompensated fits. Also, both fidelity and cross-coupling are worse for larger obscurations. Similar results are obtained for Zernike modes astigmatism and coma.

## 2. PLATE DESIGN PARAMETER VARIATIONS

In addition to the rather basic parameter variations described above, one of the purposes of the parametric study was to investigate the performance sensitivity of various possible Hartmann plate designs to variations in the input aberration characteristics. Time constraints prohibited a full design sensitivity study, but some preliminary conclusions may be drawn from the limited number of cases it was possible to run.

Three specific input beam aberration cases were provided by AFWL for analysis in this part of the parametric study. Each aberration case is described by a set of Zernike polynomial coefficient, together with a turbulence strength parameter normalized to the input beam wavelength. For each of the three aberration cases, the parametric study varied the turbulence correlation length and the Hartmann plate resolution. The performance measure for this study was Zernike mode fidelity. That is, the principal question of interest was how well the Hartmann sensors could pick out the Zernike aberration content from the turbulence (noise).

The turbulence strengths were described by the quantity  $\sigma/\lambda$ , where  $\lambda$  is the input beam wavelength and  $\sigma$  is the standard deviation of a Gaussian probability distribution describing the random (turbulent) component of the

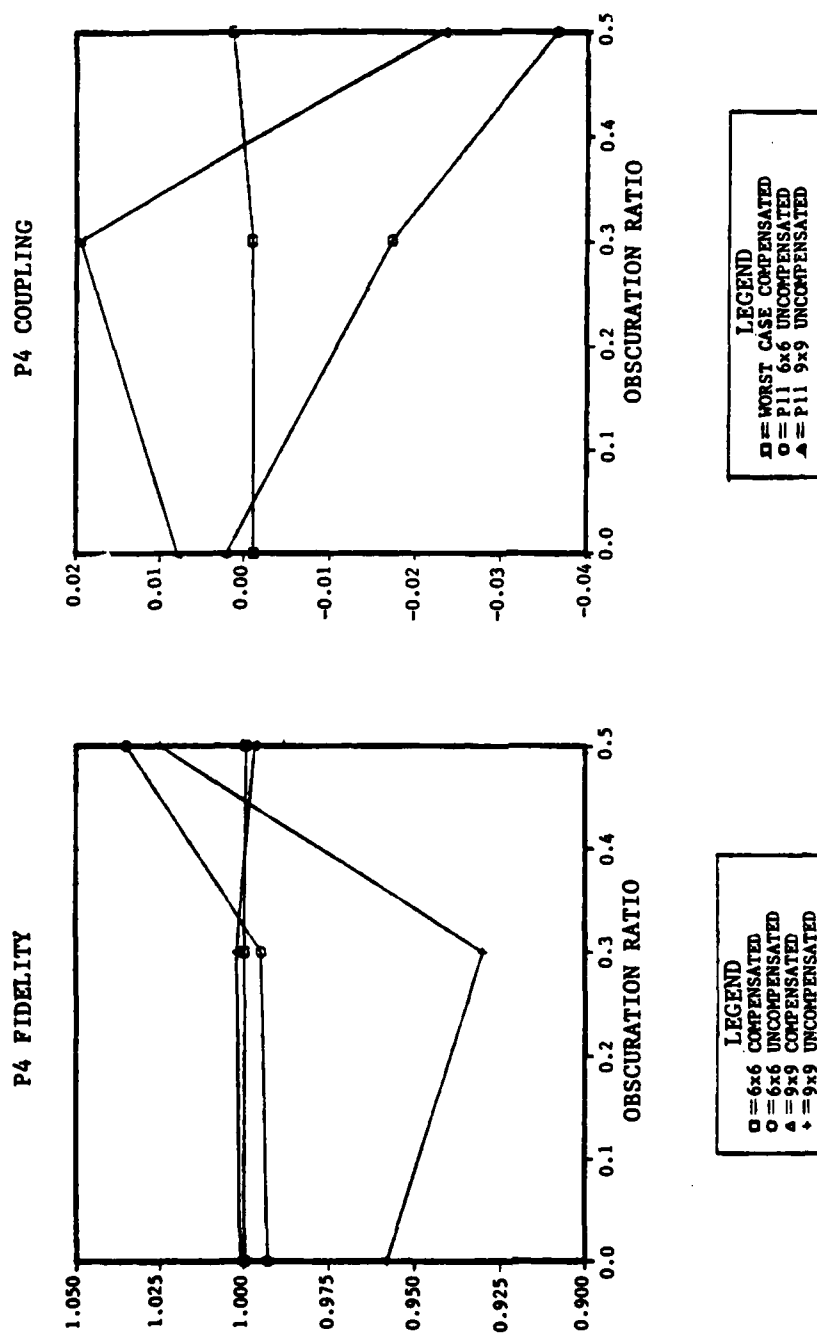


Figure 6. Effect of obscuration.

phase. Values of  $\sigma/\lambda = 0.13$ ,  $0.39$ , and  $1.04$  were prescribed. Using the range of  $\pm 3\sigma$  as a practical bound on the random wavefront variation, one finds that the values of  $\sigma/\lambda$  given correspond to expected peak-to-valley wavefront variations of about  $0.78$ ,  $2.34$ , and  $6.24$  waves. In what follows, these cases are referred to as Moderate, Strong and Severe turbulence cases, respectively.

a. Moderate Turbulence ( $\sigma/\lambda = 0.13$ ) — The input Zernike coefficients prescribed by AFWL corresponding to this case were:  $p_4 = 1.243$ ,  $p_5 = 1.217$ ,  $p_{11} = 0.067$ ,  $p_{12} = 0.060$  and  $p_{14} = 0.012$ . It is noteworthy that only  $p_4$  and  $p_5$  in this case yield peak-to-valley variations greater than the noise (turbulence) level.

Figure 7 shows the mode fidelity results for a  $1.0$ -cm correlation radius applied to the random phase. Only four random phase realizations were used. The  $12 \times 12$  - subaperture Hartmann array gives remarkably good phase fidelity in view of the fact that the signal-to-noise ratios for  $p_{11}$  and  $p_{12}$  are on the order of  $0.1$ ; i.e. the input signal for those modes is only one tenth as strong as the noise. While these are very preliminary results, they do suggest that, for moderately strong turbulence conditions and relatively short correlation lengths, very respectable performance might be achieved with a  $12 \times 12$  - subaperture Hartmann array and a small number of data samples.

Results for longer correlation radii ( $2.5$  and  $5.0$  cm) did not clearly show convergence toward fidelity values of  $1.0$ , indicating that much larger data samples (numbers of random phase realizations) are probably required in order for the statistics to settle.

b. Strong Turbulence ( $\sigma/\lambda = 0.39$ ) — The input Zernike coefficient prescribed for this case were:  $P_2 = 5.653$ ,  $p_4 = 0.333$ ,  $p_5 = 0.505$ ,  $p_7 = 0.451$ ,  $p_9 = 0.068$ ,  $p_{11} = 0.024$ ,  $p_{12} = 0.028$ , and  $p_{16} = 0.022$ . The  $\pm 3\sigma$  range for the turbulence is  $2.34$  waves peak-to-valley. Thus the input Zernike coefficients correspond to signal-to-noise ratios ranging from a maximum of  $2.4$  for  $p_2$  to a minimum of  $0.009$  for  $p_{16}$ .

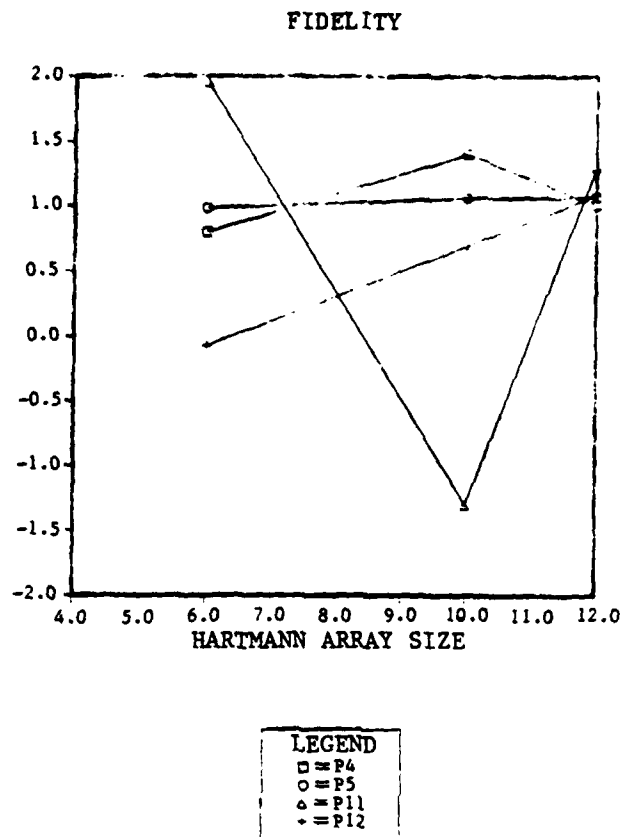


Figure 7. Phase fidelity with moderate turbulence.

Figure 8 shows the Zernike mode fidelity results for four phase realizations with a correlation radius of 1.0 cm. Only the tilt term ( $p_2$ ) shows consistently good fidelity, suggesting that larger numbers of phase realizations are probably required in this case.

c. Severe Turbulence ( $\sigma/\lambda = 1.04$ ) — The input Zernike coefficients prescribed for this case were:  $p_2 = 0.274$ ,  $p_{11} = 0.361$  and  $p_{16} = 0.012$ . The  $\pm 3\sigma$  range for the turbulence is 6.24 waves peak-to-valley. Hence, the input Zernike coefficients correspond to signal/noise ratios ranging from a maximum of 0.12 to  $p_4$  to a minimum of 0.002 for  $p_{16}$ .

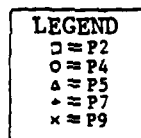
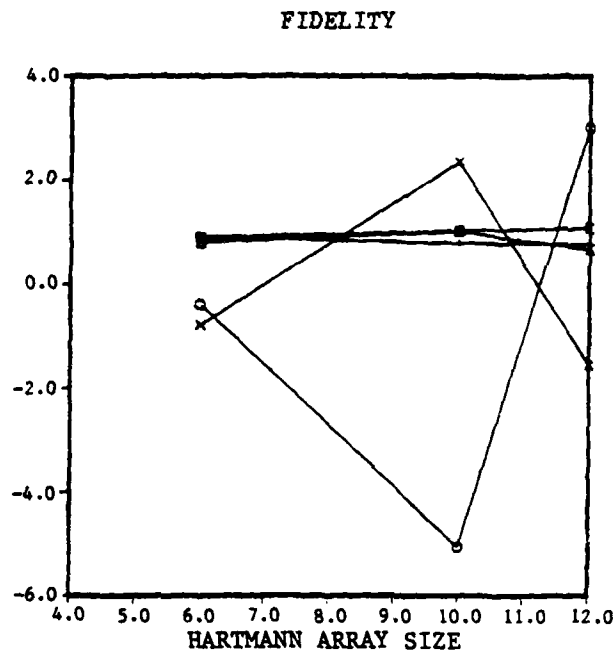


Figure 8. Phase fidelity with strong turbulence.

The Zernike mode fidelity results for this case were quite scattered, with only the tilt term ( $p_2$ ) exhibiting any consistency for a correlation radius of 1.0 cm. The input signal for this case appears to be effectively submerged in the noise, and probably only very large numbers of realizations would provide any reasonable mode fidelity. For correlation radii of 2.5 and 5.0 cm, all modes appear to be lost in the noise.

## V. CONCLUSIONS

### 1. CODE PERFORMANCE

a. Validation Test Cases — The Hartmann sensor code developed under this contract effort meets the performance specifications set forth in the SOW. In many cases, the code performance far exceeds the specifications.

b. Partial Illumination — The effects of partially illuminated subapertures on Zernike polynomial fitting and phase reconstruction may be significant for Hartmann arrays with relatively few subapertures. Increased resolution tends to reduce the errors associated with these effects. Even for very coarse (i.e.,  $3 \times 3$ ) Hartmann arrays, partial illumination effects can be very satisfactorily compensated for in the Zernike fitting algorithm, provided that the subaperture centroids of illumination can be accurately estimated. The gradient-phase reconstruction algorithm presently implemented in the simulation code, however, is not so readily adaptable to non-uniformly distributed data.

c. Correlation Random Phase — The algorithms used in generating Gaussian random phase with Gaussian correlation properties appear to perform in a satisfactory manner. Some slight spreading has been consistently observed in the correlation function re-extracted from correlated random phase realizations. While a thorough investigation of this behavior has not been performed, it is strongly suspected that the spreading is a simple consequence of the effective truncation of the Gaussian correlation function in the FFT process.

### 2. PARAMETRIC STUDY

a. Zernike Mode Fidelity — Hartmann arrays of  $12 \times 12$  or more subapertures give very reasonable Zernike mode fidelity, especially if the algorithm is permitted to compensate for partially illuminated subapertures.



b. Plate Design Parameter Variations — Only very limited conclusions are possible from this brief study. For correlation lengths which are short relative to the subaperture size, the Hartmann array appears to filter the noise component fairly efficiently. It succeeds in extracting with good fidelity Zernike modes as small as one tenth of the noise level. In those cases for which the correlation length nearly matches the subaperture size, however, it appears that large numbers of random phase realizations are probably required in order to extract the Zernike modes with reasonable fidelity, even for input Zernike modes with signal-to-noise ratios greater than 1.0.

## VI. RECOMMENDATIONS

### 1. GENERALIZED PHASE RECONSTRUCTION ALGORITHM

In order to take advantage of the phase fidelity improvements made possible by compensating for partially illuminated subapertures, it may be desirable to investigate more general approaches to phase reconstruction algorithms. This would especially be true if the expected values of random phase strength and correlation radius would tend to drive the Hartmann array design toward relatively few subapertures.

### 2. EXPANDED PARAMETRIC STUDY

Time constraints limited the parametric studies possible within this contract effort. Better understanding of the impact on sensor performance of the various design and input beam parameters really requires a much more detailed analysis than that which could be provided in this effort.